Theor Chem Acc (2006) 116: 524–534
DOI 10.1007/s00214-006-0090-8

REGULAR ISSUE

Sylvain Capponi

Effective Hamiltonian approach for strongly correlated systems

Received: 12 October 2004 / Accepted: 11 March 2005 / Published online: 14 February 2006
© Springer-Verlag 2006

Abstract We demonstrate the utility of effective Hamiltonians for studying extended correlated systems, such as quantum spin systems. After defining local relevant degrees of freedom, the numerical contractor renormalization (CORE) method is applied in two steps: (i) building an effective Hamiltonian with longer ranged interactions up to a certain cut-off using the CORE algorithm and (ii) solving this new model numerically on finite clusters by exact diagonalization and performing finite-size extrapolations to obtain results in the thermodynamic limit. This approach, giving complementary information to analytical treatments of the CORE Hamiltonian, can be used as a semi-quantitative numerical method. For ladder type geometries, we explicitly check the accuracy of the effective models by increasing the range of the effective interactions until reaching convergence. Our results in the perturbative regime and also away from it are in good agreement with previously established results. In two dimensions we consider the plaquette lattice and the *kagomé* lattice as non-trivial test cases for the numerical CORE method. As it becomes more difficult to extend the range of the effective interactions in two dimensions, we propose diagnostic tools (such as the density matrix of the local building block) to ascertain the validity of the basis truncation. On the plaquette lattice we have an excellent description of the system in both the disordered and the ordered phases, thereby showing that the CORE method is able to resolve quantum phase transitions. On the *kagomé* lattice we find that the previously proposed twofold degenerate $S = 1/2$ basis can account for a large number of phenomena of the spin $1/2$ *kagomé* system. In general, we are able to simulate system sizes which correspond to an 8×8 lattice for the plaquette lattice or a 48-site *kagomé* lattice, which are beyond the possibilities of a standard exact diagonalization approach.

PACS 75.10.Jm · 75.40.Mg · 75.40.Cx

S. Capponi
Laboratoire de Physique Théorique, CNRS UMR 5152
Université Paul Sabatier, F-31062 Toulouse, France
E-mail: sylvain.capponi@irsamc.ups-tlse.fr
Tel.: +33-561-556-840
Fax: +33-561-556-065

1 Introduction

Low-dimensional quantum magnets are the heart of current interest in strongly correlated electron systems. These systems are driven by strong correlations and large quantum fluctuations – especially when frustration comes into play – and can exhibit various unconventional phases and quantum phase transitions.

One of the major difficulties in trying to understand these systems is that strong correlations often generate highly non trivial low-energy physics. Not only the groundstate of such models is generally not known but also the low-energy degrees of freedom cannot be identified easily. Moreover, among the techniques available to investigate these systems, not many have the required level of generality to provide a systematic way to derive low-energy effective Hamiltonians.

Recently, the contractor renormalization (CORE) method has been introduced by Morningstar and Weinstein [2, 3]. The key idea of the approach is to derive an effective Hamiltonian acting on a truncated local basis set, so as to exactly reproduce the low energy spectrum. In principle the method is exact in the low energy subspace, but only at the expense of having a priori long range interactions. The method becomes most useful when one can significantly truncate a local basis set and still restrict oneself to short range effective interactions. This however depends on the system under consideration and has to be checked systematically. Since its inception the CORE method has been mostly used as an analytical method to study strongly correlated systems [4–6]. Some first steps in using the CORE approach and related ideas in a numerical framework have also been undertaken [7–9], including also the work by Jean-Paul Malrieu et al. [10, 1].

The purpose of the present paper is to give a small overview of real space renormalization ideas and then explore the numerical CORE method as a complementary approach to more analytical CORE procedures, and to discuss its performance in a variety of low dimensional quantum magnets, both frustrated and unfrustrated. The approach consists basically of numerical exact diagonalizations of the effective Hamiltonians. In this way a large number of interesting quantities

are accessible, which otherwise would be hard to obtain. Furthermore, we discuss some criteria and tools useful to estimate the quality of the CORE approach. More technical details can be found in a work done in collaboration with Läuchli and Mambrini [11].

The outline of the paper is as follows. In Sect. 1, we will discuss the low-energy emerging degrees of freedom. Then, we will review the CORE algorithm in general and discuss some particularities in a numerical CORE approach, both at the level of the calculation of the effective Hamiltonians and the subsequent simulations.

In Sect. 4 we move to the first applications on one-dimen sional (1D) systems: the Heisenberg spin chain, the well known two-leg spin ladder and the 3-leg spin ladder with periodic boundary conditions in the transverse direction (3-leg torus). We will show that the numerical CORE method is able to get rather accurate estimates of the groundstate energy and the spin gap by successively increasing the range of the effective interactions.

In Sect. 5 we discuss two-dimensional (2D) systems. As in 2D a long ranged cluster expansion of the interactions is difficult to achieve on small clusters, we will discuss some techniques to analyze the quality of the basis truncation. We illustrate these issues on two model systems, the plaquette lattice and the *kagomé* lattice. The plaquette lattice is of particular interest as it exhibits a quantum phase transition from a disordered plaquette state to a long range ordered Néel antiferromagnet, which cannot be reached by a perturbative approach. We show that a range-two effective model captures many aspects of the physics over the whole range of parameters. The *kagomé* lattice on the other hand is a highly frustrated lattice built of corner-sharing triangles and it is one best-known candidate systems for a spin liquid groundstate. A very peculiar property is the exponentially large number of low-energy singlets in the magnetic gap. We show that already a basic range two CORE approach is able to devise an effective model which exhibits the same exotic low-energy physics.

In Sect. 6, we conclude and give some perspectives.

2 Low-energy emerging degrees of freedom

In various fields, the high-energy description can be well captured by a well-known model, such as the Hubbard model in the context of high temperature superconductors. However, one is interested in low-energy properties, or similarly long-distance behaviour, which can be difficult to compute numerically since one is always limited by the size of the system. A typical situation is shown in Fig. 1

Another well-known example is given by looking at the structure of a molecule. In Fig. 2, we show that starting from a very fundamental description in terms of quarks and leptons, which is valid at high-energy, one can derive a variety of different descriptions (nucleons, atoms and finally molecule), each of them being valid at a certain energy scale.

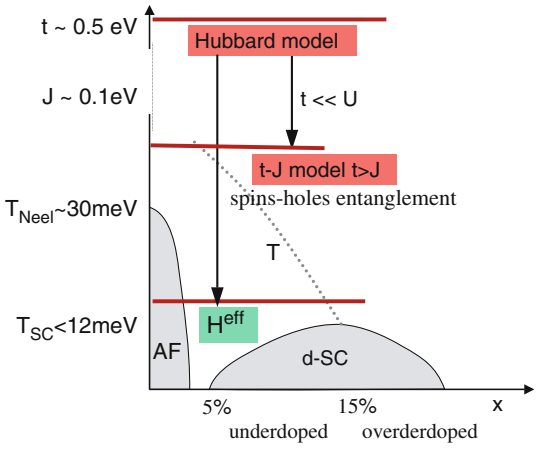

Fig. 1 Sketch of a typical high T_c cuprate phase diagram with temperature versus doping x. At high energy, it can be described by a Hubbard-like model with hopping $t \sim 0.5\,\mathrm{eV}$ and Coulomb interaction $U \sim 10\,\mathrm{eV}$. When reducing the energy scale, this model can be simplified first into a t-J model, where the magnetic scale J is given by $4t^2/U \sim 0.1\,\mathrm{eV}$. Ultimately, one is interested in the very low energy properties (few millielectron volts) where appears an antiferromagnetic phase (AF) or the famous d-wave superconductivity (d-SC). However, such an effective model H_{eff} is still not known and strongly debated

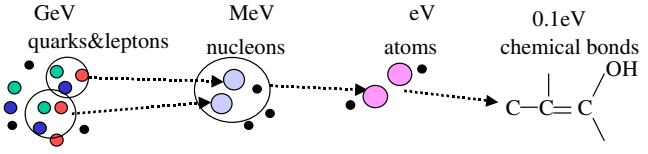

Fig. 2 Depending on the energy scale, one can choose a different description for the same object: a single molecule can be described either in terms of quarks, or nucleons, or atoms, or finally using chemical bonds concepts

The spirit of real-space renormalization group is that one can integrate out local degrees of freedom (i.e. high-energy) in order to derive an effective model which will be valid on larger distances.

The definition of relevant degrees of freedom at a given energy scale is a very deep concept in the sense that one can forget many irrelevant details and derive an effective theory. For instance, chemists know very well that an atom or a molecule are very powerful concepts, even though they do not exist as fundamental particles!

In order to conclude this section, I would like to emphasize that this last example does not mean that a theory of everything could be simply derived from particle physics knowledge. On the contrary, when dealing with a large assembly of particles, as happens in condensed matter, new relevant degrees of freedom can also emerge at low-energy and these are the relevant objects one should deal with. This idea is very nicely explained by Laughlin and Pines [12].

Going back to our purpose, a typical situation is shown in Fig. 3 in which the system size is too small to observe a finite correlation length ξ but still, the local "atoms" can have a much smaller size $\xi_{\mathrm{coherence}}$.

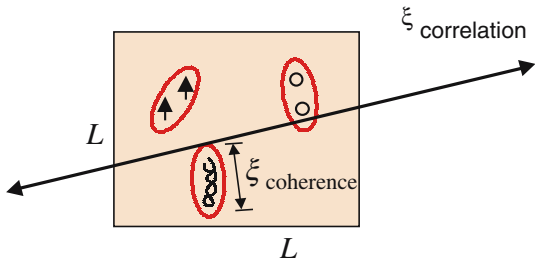

Fig. 3 A typical situation where the correlation length ξ exceeds the size of the system L. However local degrees of freedom can have a smaller coherence length $\xi_{\text{coherence}}$

The question is now to know how do we identify our relevant "atoms" and how do we compute an effective theory? The answer is provided by the CORE algorithm.

3 CORE algorithm

The CORE method has been proposed by Morningstar and Weinstein in the context of general Hamiltonian lattice models [2,3]. Later, Weinstein applied this method with success to various spin chain models [4]. For a review of the method we refer the reader to these original papers [1–3] and also to a pedagogical article by Altman and Auerbach [5] which includes many details. Here, we summarize the basic steps before discussing some technical aspects which are relevant in our numerical approach.

CORE Algorithm:

- Choose a small cluster (e.g. rung, plaquette, triangle, etc) and diagonalize it. Keep M suitably chosen low-energy states.
- Diagonalize the full Hamiltonian H on a connected graph consisting of N_c clusters and obtain its low-energy states $|n\rangle$ with energies ε_n.
- The eigenstates $|n\rangle$ are projected on the tensor product space of the states kept and Gram–Schmidt orthonormalized in order to get a basis $|\psi_n\rangle$ of dimension M^{N_c}. As it may happen that some of the eigenstates have zero or very small projection, or vanish after the orthogonalization it might be necessary to explicitly compute more than just the lowest M^{N_c} eigenstates $|n\rangle$.
- Next, the effective Hamiltonian for this graph is built as

$$h_{N_c} = \sum_{n=1}^{M^{N_c}} \varepsilon_n |\psi_n\rangle\langle\psi_n|. \tag{1}$$

- The connected range-N_c interactions $h_{N_c}^{\text{conn}}$ are determined by substracting the contributions of all connected subclusters.
- Finally, the effective Hamiltonian is given by a cluster expansion as

$$H^{\text{CORE}} = \sum_i h_i + \sum_{\langle ij\rangle} h_{ij} + \sum_{\langle ijk\rangle} h_{ijk} + \cdots . \tag{2}$$

This effective Hamiltonian *exactly* reproduces the low-energy physics provided the expansion goes to infinity. However, if the interactions are short-range in the starting Hamiltonian, we can expect that these operators will become smaller and smaller, at least in certain situations (it depends on the emerging $\xi_{\text{coherence}}$ length). In the following, we will truncate at range r and verify the convergence in several cases. This convergence naturally depends on the number M of low-lying states that are kept on a basic block. In order to describe quantitatively how "good" these states are, we introduce the density matrix in Sect. 5.

In the present work, we investigate mainly SU(2) invariant Heisenberg models described by the usual Hamiltonian

$$H = \sum_{\langle ij\rangle} J_{ij} \mathbf{S}_i \cdot \mathbf{S}_j \tag{3}$$

where the exchange constants J_{ij} will be limited to short-range distances in the following.

Once an effective Hamiltonian has been obtained, it is still a formidable task to determine its properties. Within the CORE method different routes have been taken in the past. In their pioneering papers, Morningstar and Weinstein have chosen to iteratively apply the CORE method on the preceding effective Hamiltonian in order to flow to a fixed point and then to analyze the fixed point. A different approach has been taken in Refs. [4, 5] : There the effective Hamiltonian after one or two iterations has been analyzed with mean-field like methods and interesting results have been obtained. Yet another approach – and the one we will pursue in this paper – consists of a single CORE step to obtain the effective Hamiltonian, followed by a numerical simulation thereof. This approach has been explored in few previous studies [6–8]. The numerical technique we employ is the exact diagonalization (ED) method based on the Lanczos algorithm. This technique has easily access to many observables and profits from the symmetries and conservation laws in the problem, i.e. total momentum and the total S^z component. Using a parallelized program we can treat matrix problems of dimensions up to $\sim$ 50 millions, however the matrices contain significantly more matrix elements than the ones of the microscopic Hamiltonian we start with.

4 Chain and ladder geometries

In this section, we describe results obtained on $S = 1/2$ spin chain and ladder systems with 2 and 3 legs, respectively.

We want to build an effective model that is valid from a perturbative regime to the isotropic case $J_{ij} = J = 1$. We have chosen periodic boundary conditions (PBC) along the chains in order to improve the convergence to the thermodynamic limit.

4.1 1D Heisenberg chain

In this simple example, one is able to iterate the CORE procedure in order to obtain the ground-state energy. Let us recall

that this model has an exact solution for the ground-state energy $e_0 = -\ln 2 + 1/4$ and has an infinite correlation length so that a numerical approach on a finite system is not obvious. Using CORE and solving up to 12 sites, which is very easy even on a small computer, Weinstein has obtained [3] a ground-state energy which is correct at 10^{-5}!

A similar idea consists of increasing the size of the initial block, instead of the range of effective interactions, and this has been applied by Jean-Paul Malrieu et al. to the same system [9]. Solving numerically up to 22 sites, they have a relative error of 10^{-4}.

Being able to obtain such an accuracy on a ground-state energy by solving small systems compared to the infinite correlation length is very encouraging. Therefore, we have pursued this approach more systematically on other models.

4.2 Two-leg Heisenberg ladder

The two-leg Heisenberg ladder has been intensively studied and is known to exhibit a spin gap for all couplings [13–16].

In order to apply our algorithm, we select a 2×2 plaquette as the basic unit (see Fig. 4a). The truncated subspace is formed by the singlet ground-state (GS) and the lowest triplet state.

Using the same CORE approach, Piekarewicz and Shepard [6] have shown that quantitative results can be obtained within this restricted subspace. Moreover, dynamical quantities can also be computed in this framework [7].

Since we are dealing with a simple system, we can compute the effective models including rather long-range interactions (typically, to obtain range-4 interactions, we need to compute the low-lying states on a 2×8 lattice with open boundary conditions which is feasible, although it requires a large numerical effort). It is desirable to compute long-range effective interactions since we wish to check how the truncation affect the physical results and how the convergence is reached.

In a second step, for each of these effective models, we perform a standard exact diagonalization (ED) using the Lanczos algorithm on finite clusters up to $N_c = 12$ clusters ($N = 48$ sites for the original model). The GS energy and the spin gap are shown in Fig. 5. The use of PBC allows to reduce considerably finite-size effects since we have an exponential

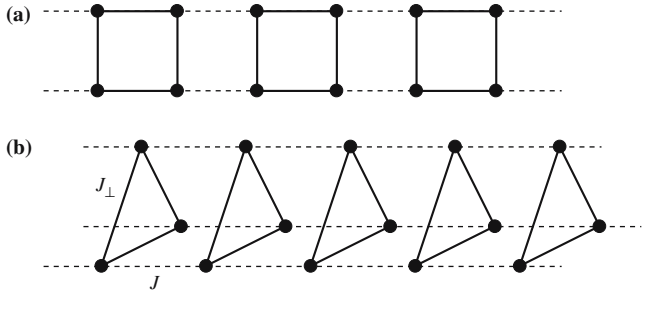

Fig. 4 **a** Two-leg ladder. Basic block is a 2×2 plaquette. **b** Three-leg torus with rung coupling $J_\perp$ and inter-rung coupling $J_\parallel$

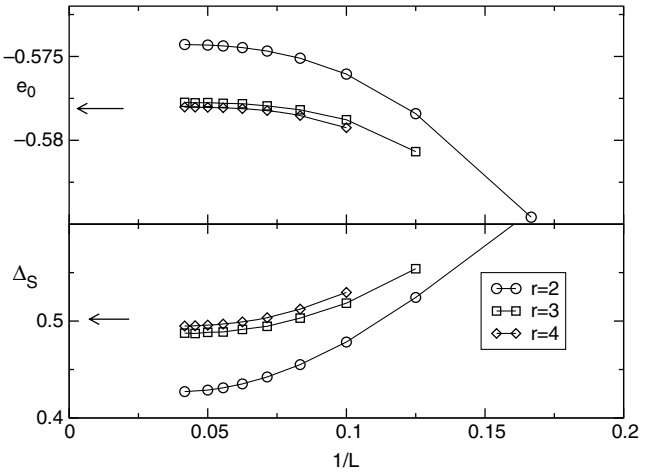

Fig. 5 Ground-state energy per site and spin gap of a $2 \times L$ Heisenberg ladder using CORE method with various range r using PBC. For comparison, we plot the best known extrapolations [14–16] with *arrows*

convergence as a function of inverse length. CORE results are in perfect agreement with known results and the successive approximations converge uniformly to the exact results. For instance, the relative errors of range-4 results are 10^{-4} for the GS energy and 10^{-2} for the spin gap. This fast convergence is probably due to the rather short correlation length in an isotropic ladder (typically 3 to 4 lattice spacings [17]).

4.3 Three-leg Heisenberg torus

As a second example of ladder geometry, we have studied a three-leg Heisenberg ladder with PBC along the rungs. This property causes geometric frustration which leads to a finite spin-gap and finite dimerization for all interchain coupling $J_\perp$ [18,19], contrary to the open boundary condition case along the rungs, which is in the universality class of the Heisenberg chain.

Perturbation theory : The simple perturbation theory is valid when the coupling along the rung ($J_\perp$) is much larger than between adjacent rungs ($J_\parallel$). In the following, we fix $J_\perp = 1$ as the energy unit and denote $\alpha = J_\parallel / J_\perp$.

On a single rung, the low-energy states are the following degenerate states, defined as

$$
\begin{aligned}
|\uparrow L\rangle &= \frac{1}{\sqrt{3}}(|\uparrow\uparrow\downarrow\rangle + \omega\,|\uparrow\downarrow\uparrow\rangle + \omega^2\,|\downarrow\uparrow\uparrow\rangle),\\
|\downarrow L\rangle &= \frac{1}{\sqrt{3}}(|\downarrow\downarrow\uparrow\rangle + \omega\,|\downarrow\uparrow\downarrow\rangle + \omega^2\,|\uparrow\downarrow\downarrow\rangle),\\
|\uparrow R\rangle &= \frac{1}{\sqrt{3}}(|\uparrow\uparrow\downarrow\rangle + \omega^2\,|\uparrow\downarrow\uparrow\rangle + \omega\,|\downarrow\uparrow\uparrow\rangle),\\
|\downarrow R\rangle &= \frac{1}{\sqrt{3}}(|\downarrow\downarrow\uparrow\rangle + \omega^2\,|\downarrow\uparrow\downarrow\rangle + \omega\,|\uparrow\downarrow\downarrow\rangle)
\end{aligned}
\tag{4}
$$

where $\omega = \exp(i2\pi/3)$. The indices L and R represent the momentum of the three-site ring $k_y = 2\pi/3$ and $-2\pi/3$,

respectively. They define two chiral states which can be viewed as pseudo-spin states with operators $\boldsymbol{\tau}$ on each rung defined by

$$\tau^+ \mid \cdot R\rangle = 0, \quad \tau^+ \mid \cdot L\rangle = \mid \cdot\ R\rangle,$$
$$\tau^- \mid \cdot R\rangle = \mid \cdot\ L, \rangle \quad \tau^- \mid \cdot L\rangle = 0,$$
$$\tau^z \mid \cdot R\rangle = \frac{1}{2} \mid \cdot R\rangle, \quad \tau^z \mid \cdot L\rangle = -\frac{1}{2} \mid \cdot L\rangle$$

These states have in addition a physical spin 1/2 described by $\boldsymbol{\sigma}$.

Applying the usual perturbation theory for the inter-rung coupling, one finds[18,20]:

$$H_{\text{pert}} = -\frac{N}{4} + \frac{\alpha}{3} \sum_{\langle ij \rangle} \boldsymbol{\sigma}_i \cdot \boldsymbol{\sigma}_j (1 + 4(\tau_i^+ \tau_j^- + \tau_i^- \tau_j^+)) \quad (5)$$

where N is the total number of sites.

This effective Hamiltonian has been studied with DMRG and ED techniques and it exhibits a finite spin gap $\Delta_S = 0.28\ J_\parallel$ and a dimerization of the ground state [18,19].

Here, we want to use the CORE method to extend the perturbative Hamiltonian with an effective Hamiltonian in the same basis for *any* coupling.

CORE approach : As a basic unit, we choose a single three-site rung. The subspace consists of the same low-energy states as for the perturbative result [Eq. (4)] which are four-fold degenerate (two degenerate $S = 1/2$ states). We can apply our procedure to compute the effective interactions at various ranges, in order to be able to test the convergence of the method.

In order to study how the physical properties evolve as a function of $J_\parallel/J_\perp$, we have computed the GS energy and the spin gap, both for a small-coupling case and in the isotropic limit, up to range 5 in the effective interactions.

Small interrung coupling : We have chosen $J_\parallel/J_\perp = 0.25$ which corresponds to a case where perturbation theory should still apply. Using ED, we can solve the effective models on finite lattices and in Fig. 6, we plot the scaling of the GS energy and of the spin gap as a function of the system length L. Even for this rather small value of $J_\parallel/J_\perp$, our effective Hamiltonian can be considered as an improvement over the first order perturbation theory. Moreover, we observe a fast convergence with the range of interactions and already the range-3 approximation is almost indistinguishable from ED results.

The estimated gap is $0.16J_\parallel$ and correspond to a lower bound since ultimately the gap should converge exponentially to its thermodynamic value. Our value is consistent with the DMRG one [18] ($\sim 0.2J_\parallel$), and is already reduced compared to the strong coupling result [18] ($\Delta_S = 0.28J_\parallel$).

Isotropic case : We apply the same procedure in the isotropic limit. As expected, the convergence with the range of interactions is much slower than in the perturbative regime. We show in Fig. 7 that indeed the ground state energy converges slowly and oscillates around the correct value. These oscillations come from the fact that, in order to compute range-r interactions, one has to study alternatively clusters

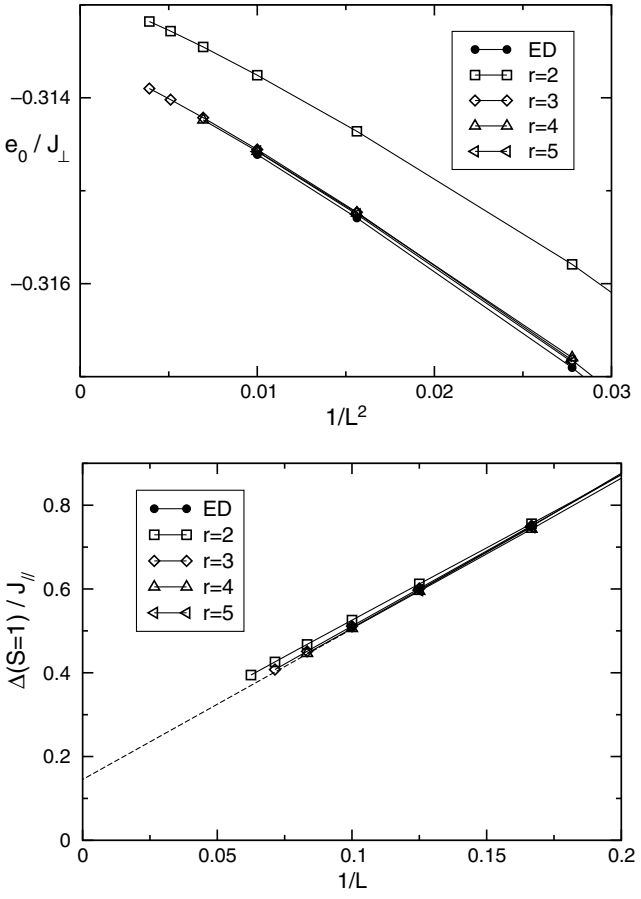

Fig. 6 Ground-state (GS) energy per site and spin gap for a $3 \times L$ Heisenberg torus with $J_\parallel/J_\perp = 0.25$. Results are obtained using the CORE method at various ranges r

with an even or odd number of sites. Since this system has a tendency to form dimers on nearest-neighbour bonds, it is better to compute clusters with an even number of sites.

For the spin gap, we find accurate results even with limited range interactions. In particular, we find that frustration induces a finite spin gap $\simeq 0.11\ J_\parallel$ in that system. As in the previous case, this is a lower bound which is in perfect agreement with DMRG study [18].

Moreover, we observe that the singlet gap vanishes in the thermodynamic limit as $1/L^2$ (data not shown), similar to a related study [19]. This singlet state at momentum π along the chains corresponds to the state built in the generalized Lieb–Schultz–Mattis argument [21,22]. Here, the physical picture is a twofold degenerate GS due to the appearance of spontaneous dimerization.

Therefore, with CORE method, we have both the advantage of working in the reduced subspace and not being limited to the perturbative regime. Amazingly, we have observed that for a very small effort (solving a small cluster), the effective Hamiltonian gives much better results (often less than 1% on GS energies) than perturbation theory. It also gives an easier framework to systematically improve the accuracy by including longer range interactions.

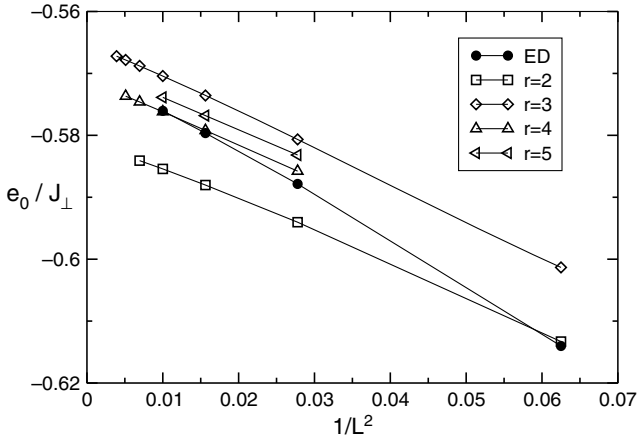

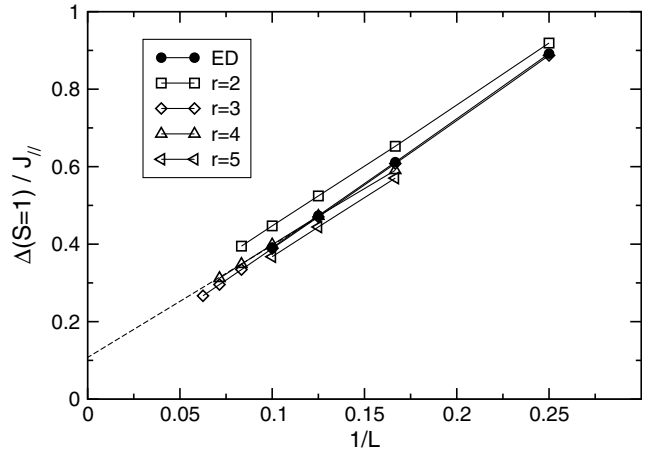

Fig. 7 Same as Fig. 6 for the isotropic case $J_{\parallel} = J_{\perp} = 1$

For these models, the good convergence of CORE results may be due to the fact that the GS in the isotropic limit is adiabatically connected to the perturbative one. In the following part, we will therefore study 2D models where a quantum phase transition occurs as one goes from the perturbative to the isotropic regime.

5 Two dimensional spin models

In this section, we would like to discuss the application of the numerical CORE method to two-dimensional quantum spin systems. We will present spectra and observables and also discuss a novel diagnostic tool – the density matrix of local objects – in order to justify the truncation of the local state set.

One major problem in two dimension is the more elaborate cluster expansion appearing in the CORE procedure. Especially, our approach based on numerical diagonalization of the resulting CORE Hamiltonian faces problems once the CORE interaction clusters wrap around the boundary of the finite size clusters. We therefore try to keep the range of the interactions minimal, but we still demand a reasonable description of low energy properties of the system. We will therefore discuss some ways to detect under what circumstances the low-range approximations fail and why.

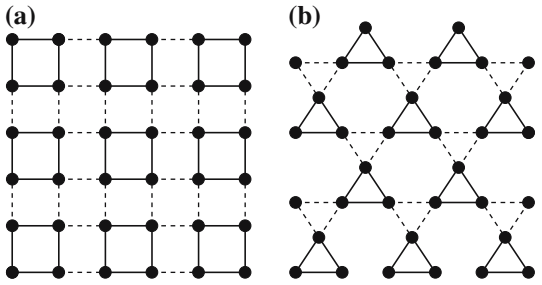

Fig. 8 **a** The plaquette lattice. *Full lines* denote the plaquette bonds J, *dashed lines* denote the inter-plaquette coupling J'. **b** The trimerized *kagomé* lattice. *Full lines* denote the up-triangle J bonds, *dashed lines* denote the down-triangle coupling J'. The standard *kagomé* lattice is recovered for $J'/J = 1$

As a first example, we discuss the plaquette lattice (Fig. 8(a)), which exhibits a quantum phase transition from a gapped plaquette-singlet state with only short ranged order to a long range ordered antiferromagnetic state as a function of the interplaquette coupling [23–26]. We will show that the CORE method works particularly well for this model by presenting results for the excitation spectra and the order parameter. It is also a nice example of an application where the CORE method is able to correctly describe a quantum phase transition, thus going beyond an augmented perturbation scheme.

The second test case is the highly frustrated *kagomé* lattice (Fig. 8(b)) with non-integer spin, which has been intensively studied for $S = 1/2$ during the last few years [27–31]. Its properties are still not entirely understood, but some of the features are well accepted by now: there is no simple local order parameter detectable, neither spin order nor valence bond crystal order. There is probably a small spin gap present and most strikingly an exponentially growing number of low energy singlets emerges below the spin gap. We will discuss a convenient CORE basis truncation which has emerged from a perturbative point of view [30,32,33] and consider an extension of this basis for higher non-integer spin.

5.1 Plaquette lattice

The CORE approach starts by choosing a suitable decomposition of the lattice and a subsequent local basis truncation. In the plaquette lattice, the natural decomposition is directly given by the uncoupled plaquettes. Among the 16 states of an isolated plaquette we retain the lowest singlet [$K = (0, 0)$] and the lowest triplet [$K = (\pi, \pi)$]. The standard argument for keeping these states relies on the fact that they are the lowest energy states in the spectrum of an isolated plaquette.

As discussed in [1], the density matrix of a plaquette in the fully interacting system gives clear indications whether the basis is suitably chosen. In Fig. 9, we show the evolution of the density matrix weights of the lowest singlet and triplet as a function of the interplaquette coupling. Even though

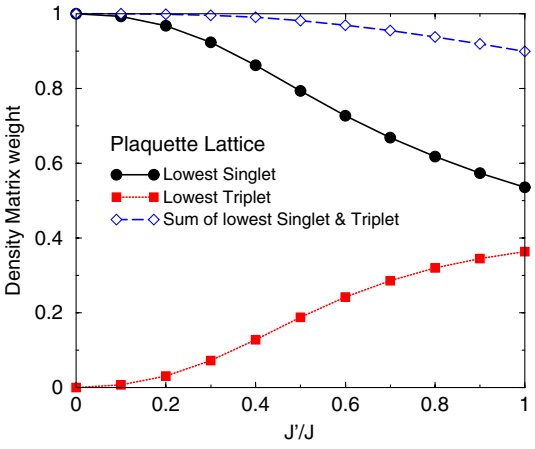

Fig. 9 Density matrix weights of the two most important states on a strong (J-bonds) plaquette as a function of J'/J. These results were obtained by ED with the original Hamiltonian on a 4×4 cluster

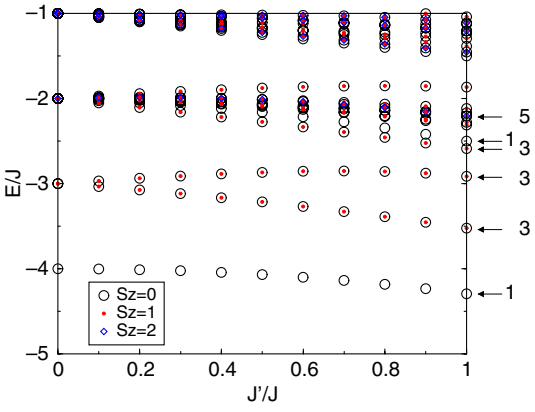

Fig. 10 Low energy spectrum of two coupled plaquettes. The states targeted by the CORE algorithm are indicated by *arrows* together with their $SU(2)$ degeneracy

the individual weights change significantly, the sum of both contributions remains above 90% for all $J'/J \leq 1$. We therefore consider this a suitable choice for a successful CORE application.

A next control step consists in calculating the spectrum of two coupled plaquettes, and one monitors which states are targeted by the CORE algorithm. We show this spectrum in Fig. 10 along with the targeted states. We realize that the 16 states of our tensor product basis cover almost all the low energy levels of the coupled system. There are only two triplets just below the $S = 2$ multiplet which are missed.

In a first application, we calculate the spin gap for different system sizes and couplings J'/J. The results shown in Fig. 11 indicate a reduction of the spin gap for increasing J'/J. We used a simple finite size extrapolation in $1/N$ in order to assess the closing of the gap. The extrapolation levels off to a small value for $J'/J \geq 0.6$. The appearance of a small gap in this known gapless region is a feature already present in ED calculation of the original model [26], and therefore *not* an artefact of our method. It is rather obvious that the triplet gap is not a very accurate tool to detect the quantum phase transition within our numerical approach. We will see later that order parameter susceptibilities are much more accurate.

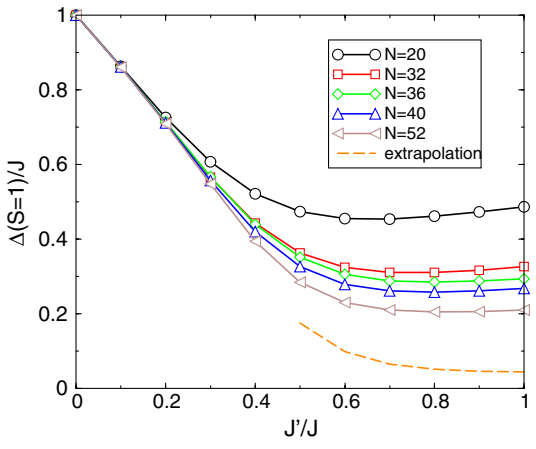

Fig. 11 Triplet gap for effective system sizes between 20 and 52 sites, as a function of the interplaquette coupling J'/J. For $J'/J \geq 0.5$ a simple extrapolation in $1/N$ is also displayed. These results compare very well with ED results on the original model [26]

It is well known that the square lattice ($J'/J = 1$) is Néel ordered. One possibility to detect this order in ED is to calculate the so-called *tower of excitation*, i.e. the complete spectrum as a function of $S(S+1)$, S being the total spin of an energy level. In the case of standard collinear Néel order a prominent feature is an alignment of the lowest level for each S on a straight line, forming a so called "quasi-degenerate joint states" (QDJS) ensemble [34], which is clearly separated from the rest of the spectrum on a finite size sample. We have calculated the tower of states within the CORE approach (Fig. 12). Due to the truncated Hilbert space we cannot expect to recover the entire spectrum. Surprisingly, however the CORE tower of states successfully reproduces

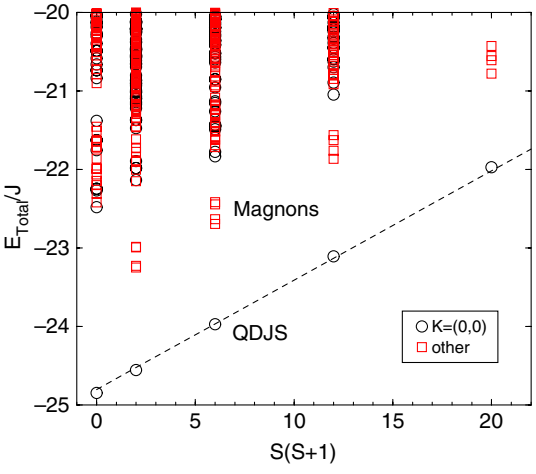

Fig. 12 Tower of states obtained with a range-two CORE Hamiltonian on an effective $N = 36$ square lattice (9-site CORE cluster) in different reduced momentum sectors. The tower of states is clearly separated from the decimated magnons and the rest of the spectrum

the general features observed in ED calculations of the same model [35]: (a) a set of QDJS with the correct degeneracy and quantum numbers (in the folded Brillouin zone); (b) a reduced number of magnon states at intermediate energies, both set of states rather well separated from the high energy part of the spectrum. While the QDJS seem not to be affected by the CORE decimation procedure, clearly some of the magnon modes get eliminated by the basis truncation.

In order to locate the quantum phase transition from the paramagnetic, gapped regime to the Néel ordered phase, a simple way to determine the onset of long range order is desireable. We chose to directly couple the order parameter to the Hamiltonian and to calculate generalized susceptibilities by deriving the energy with respect to the external coupling. Its simplicity relies on the fact that only eigenvalue runs are necessary. Similar approaches have been used so far in ED and QMC calculations [36,37].

Our results in Fig. 13 show the evolution of the staggered moment per site in a rescaled external staggered field for different inter-plaquette couplings J' and different system sizes (up to 8×8 lattices). We note the appearance of an approximate crossing of the curves for different system sizes, once Néel LRO sets in. This approximate crossing relies on the fact that the slope of $m_L(hN)$ diverges at least linearly in N in the ordered phase [37]. We then consider this crossing feature as an indication of the phase transition and obtain a value of the critical point $J_c/J = 0.55 \pm 0.05$. This estimate is in good agreement with previous studies using various methods [24–26]. We have checked the present approach by performing the same steps on the two-leg ladder discussed in Sect. 4.2 and there was no long range magnetic order present, as expected.

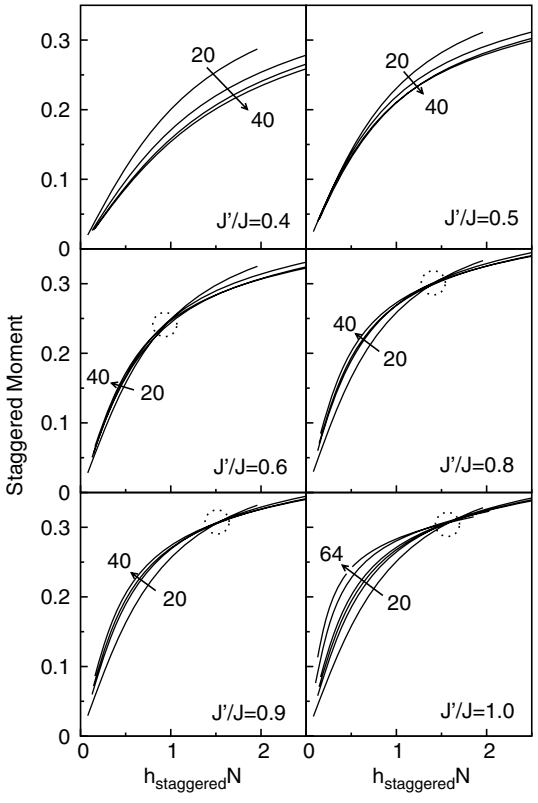

Fig. 13 Staggered moment per site as a function of the rescaled applied staggered field for the plaquette lattice and different values of J'/J. *Circles* denote the approximate crossing point of curves for different system sizes. We take the existence of this crossing as a phenomenological indication for the presence of Néel LRO. In this way, the phase transition is detected between $0.5 < J'_c/J < 0.6$, consistent with previous estimates. The *arrows* indicate curves for increasing system sizes: 20, 32, 36, 40 and also 52, 64 for the isotropic case

5.2 *kagomé* systems with half-integer spins

In the past 10 years, many efforts have been devoted to understand the low energy physics of the *kagomé* antiferromagnet (KAF) for spins 1/2 [27–31]. At the theoretical level, the main motivation comes from the fact that this model is the only known example of a two-dimensional Heisenberg spin liquid. Even though many questions remain open, some very exciting low-energy properties of this system have emerged. Let us summarize them briefly: (i) the GS is a singlet ($S = 0$) and has no magnetic order. Moreover no kind of more exotic ordering (dimer–dimer, chiral order, etc.) have been detected using unbiased methods; (ii) the first magnetic excitation is a triplet ($S = 1$) separated from the GS by a rather small gap of order $J/20$; (iii) more surprisingly the spectrum appears as a continuum of states in all spin sectors. In particular, the spin gap is filled with an exponential number of singlet excitations: $\mathcal{N}_{\text{singlets}} \sim 1.15^N$; (iv) the singlet sector of the KAF can be very well reproduced by a short-range resonating valence bond approach involving only nearest-neighbor dimers.

From this point of view, the spin 1/2 KAF with its highly unconventional low-energy physics appears to be a very sharp test of the CORE method and it was also recently studied in [39,40]. The case of higher half-integer spins $S = 3/2, 5/2, \ldots$, KAF is also of particular interest, since it is covered by approximative experimental realizations [38].

In this section, we discuss in detail the range-two CORE Hamiltonians for spin 1/2 KAF considered as a set of elementary up-triangles with couplings J, coupled by down-triangles with couplings J' (see Fig. 8(b)). The coupling ratio will be denoted by $\alpha = J'/J$.

5.2.1 Choice of the CORE basis

We decide to keep the two degenerate $S = 1/2$ doublets on a triangle for the CORE basis. In analogy to the the plaquette lattice, we calculate the density matrix of a single triangle embedded in a 12 site *kagomé* lattice, in order to get information on the quality of the truncated basis. The results show that the targeted states exhaust 95%, which indicates that the approximation seems to work particularly well, thereby providing independent support for the adequacy of the basis chosen in a related mean-field study [30].

We continue the analysis of the CORE basis by monitoring the evolution of the spectra of two coupled triangles

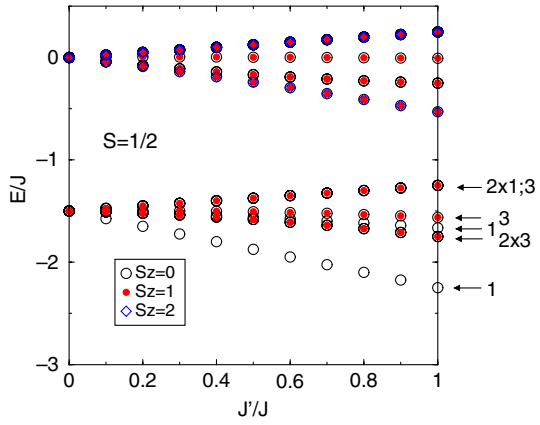

Fig. 14 Spectrum of two coupled triangles in the *kagomé* geometry with $S = 1/2$ spins. The entire lowest band containing 16 states is successfully targeted by the CORE algorithm

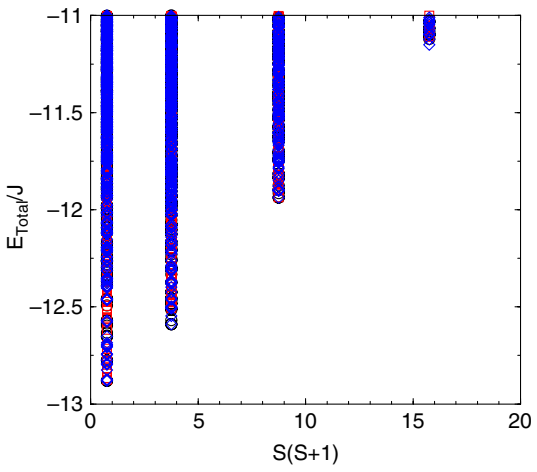

Fig. 15 Tower of states obtained with a range-two CORE Hamiltonian on an effective $N = 27$ *kagomé* lattice (9-site CORE cluster). There is a large number of low-lying states in each S sector. The *symbols* correspond to different momenta

in the *kagomé* geometry as a function of the inter-triangle coupling J', as well as the states selected by the range-two CORE algorithm. The spectrum is shown in Fig. 14. We note the presence of a clear gap between the 16 lowest states – correctly targeted by the CORE algorithm – and the higher lying bands. This can be considered an ideal case for the CORE method. Based on this and the results of the density matrix, we expect the CORE range-two approximation to work quite well.

5.2.2 Simulations for $S = 1/2$

After having studied the CORE basis and the effective Hamiltonian at range two in some detail, we now proceed to the actual simulations of the resulting model. We perform the simulations for the standard *kagomé* lattice, therefore $\alpha = 1$. We will calculate several distinct physical properties, such as the tower of excitations, the evolution of the triplet gap as a function of system size and the scaling of the number of singlets in the gap. These quantities have been discussed in great detail in previous studies of the *kagomé* $S = 1/2$ antiferromagnet [27–31].

First we calculate the tower of excitations for a *kagomé* $S = 1/2$ system on a 27 sites sample. The data is plotted in Fig. 15. The structure of the spectrum follows the exact data of [24] rather closely; i.e there is no QDJS ensemble visible, a large number of $S = 1/2$ states covering all momenta are found below the first $S = 3/2$ excitations and the spectrum is roughly bounded from below by a straight line in $S(S+1)$. Note that the tower of states we obtain here is strikingly different from the one obtained in the Néel ordered square lattice case, see Fig. 12.

Next, we calculate the spin gap using the range-two CORE Hamiltonian. Results for system sizes up to 48 sites are shown in Fig. 16, together with ED data where available. In comparison we note two observations: (a) the CORE range-two approximation seems to systematically overestimate the gap, but captures correctly the sample to sample variations, (b) the gaps of the smallest samples (effective N=12,15) deviate

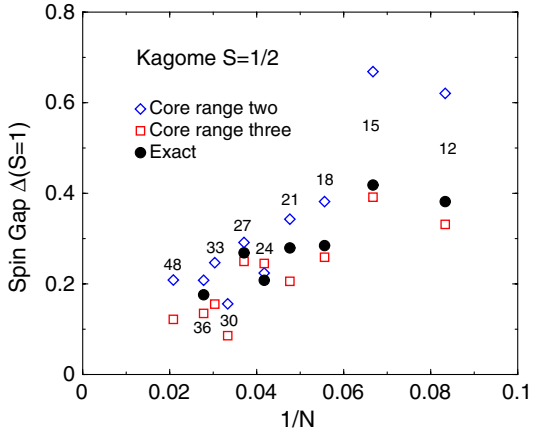

Fig. 16 Spin gap of the *kagomé* $S = 1/2$ model on various samples, obtained with the CORE method (range-two and three). Exact diagonalization result are also shown for comparison where available

strongly from the exact data. We observed this to be a general feature of very small clusters in the CORE approach. In order to improve the agreement with the ED data, we calculated the two CORE range-three terms containing a closed loop of triangles. The results obtained with this extended Hamiltonian are shown as well in Fig. 16. These additional terms improve the gap data somewhat. We now find the CORE gaps to be mostly smaller than the exact ones. The precision of the CORE gap data is not accurate enough to make a reasonable prediction on the spin gap in the thermodynamic limit. However, we think that the CORE data is compatible with a finite spin gap.

Finally, we determine the number of nonmagnetic excitations within the magnetic gap for a variety of system sizes up to 39 sites. Similar studies of this quantity in ED gave evidence for an exponentially increasing number of singlets in the gap [28,29]. We display our data in comparison to the exact results in Fig. 17. While the precise numbers are not

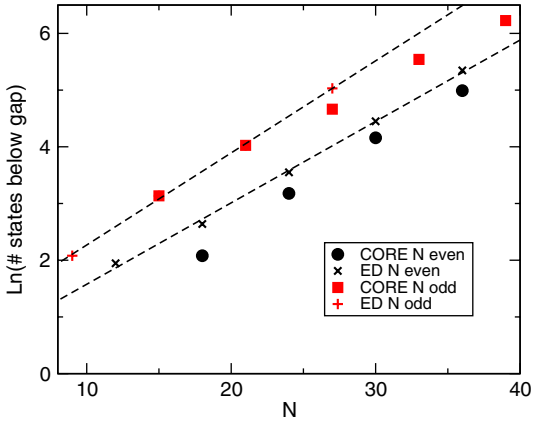

Fig. 17 Logarithm of the number of states within the magnetic gap. Results obtained with the CORE range-two Hamiltonian. For comparison exact data obtained in [28,29] are shown. The *dashed lines* are linear fits to the exact diagonalization data

expected to be recovered, the general trend is well described with the CORE results. For both even and odd N samples, we see an exponential increase of the number of these non-magnetic states. In the case of $N = 39$ for example, we find 506 states below the first magnetic excitation. These results emphasize again the validity of the two doublet basis for the CORE approach on the *kagomé* spin 1/2 system.

6 Conclusions

We have discussed the usefulness of real-space renormalization techniques – the so-called numerical CORE method – in obtaining local low-energy relevant degrees of freedom and an effective theory in the context of low-dimensional quantum magnetism. This method consists of two steps: (i) building an effective Hamiltonian acting on the low-energy degrees of freedom of some elementary block; and (ii) studying this new model numerically on finite-size clusters, using a standard ED or similar approach.

Like in other real-space renormalization techniques the effective model usually contains longer range interactions. The numerical CORE procedure will be most efficient provided the effective interactions decay sufficiently fast. We discussed the validity of this assumption in several cases.

For ladder type geometries, we explicitly checked the accuracy of the effective models by increasing the range of the effective interactions until reaching convergence. Both in the perturbative regime and in the isotropic case, our results on a two-leg ladder and a three-leg torus are in good agreement with previously established results. This rapid convergence might be due to the small correlation length in these systems which both have a finite spin gap.

In two dimensions, we have used the density matrix as a tool to check whether the restricted basis gives a good enough representation of the exact states. When this is the case, as for the plaquette lattice or the $S = 1/2$ *kagomé* lattice, the lowest order range-two effective Hamiltonian gives semi-quantitative results, even away from any perturbative regime. For example, we can successfully describe the plaquette lattice, starting from the decoupled plaquette limit through the quantum phase transition to the Néel ordered state at homogeneous coupling. Furthermore, we can also reproduce many aspects of the exotic low-energy physics of the $S = 1/2$ *kagomé* lattice.

Therefore within the CORE method, we can have both the advantage of working in a strongly reduced subspace and not being limited to the perturbative regime in certain cases.

We thus believe that the numerical CORE method can be used systematically to explore possible ways of generating low-energy effective Hamiltonians.

Acknowledgements I thank A. Läuchli and M. Mambrini for their help in this work, and I acknowledge fruitful discussions with F. Alet, A. Auerbach, J.-P. Malrieu, F. Mila and D. Poilblanc. I also thank IDRIS (Orsay) for allocation of CPU time.

References

1. Al Hajj M, Guihéry N, Malrieu J-P, Wind P (2004) Phys Rev B 70:094415
2. Morningstar CJ, Weinstein M (1994) Phys Rev Lett 73:1873
3. Morningstar CJ, Weinstein M (1996) Phys Rev D 54:4131
4. Weinstein M (2001) Phys Rev B 63:174421
5. Altman E, Auerbach A (2002) Phys Rev B 65:104508
6. Berg E, Altman E, Auerbach A (2003) Phys Rev Lett 90:147204
7. Piekarewicz J, Shepard JR (1997) Phys Rev B 56:5366
8. Piekarewicz J, Shepard JR (1998) Phys Rev B 57:10260
9. Capponi S, Poilblanc D (2002) Phys Rev B 66:180503(R)
10. Malrieu J-P, Guihéry N (2001) Phys Rev B 63:085110
11. Capponi S, Läuchli A, Mambrini M (2004) Phys Rev B
12. Laughlin RB, Pines D (2000), Proc Nat Acad Sci 97:28 (see the discussion and references)
13. Dagotto E, Rice TM (1996) Science 271:618 and references therein
14. Barnes T, Dagotto E, Riera J, Swanson ES (1993) Phys Rev B 47:3196
15. White SR, Noack RM, Scalapino DJ (1994) Phys Rev Lett 73:886
16. Frischmuth B, Ammon B, Troyer M (1996) Phys Rev B 54: R3714
17. Greven M, Birgeneau RJ, Wiese U-J (1996) Phys Rev Lett 77:1865
18. Kawano K, Takahashi M (1997) J Phys Soc Jpn 66:4001
19. Cabra DC, Honecker A, Pujol P (1998) Phys Rev B 58:6241
20. Martin T, Montambaux G, Trân Thanh Vân J (eds) (1996) In: Proceedings of the XXXIst Rencontres de Moriond, Frontières, Gif-sur-Yvette, France (cond-mat/9605075)
21. Lieb E, Schultz T, Mattis D (1961) Ann Phys 16:407
22. Affleck I (1988) Phys Rev B 37:5186
23. Koga A, Kumada S, Kawakami N (1999) J Phys Soc Jpn 68:642
24. Koga A, Kumada S, Kawakami N (1999) J Phys Soc Jpn 68:2373
25. Läuchli A, Wessel S, Sigrist M (2002) Phys Rev B 66:014401
26. Voigt A (2002) Comput Phys Commun 146:125
27. Leung PW, Elser V (1993) Phys Rev B 47:5459
28. Lecheminant P, Bernu B, Lhuillier C, Pierre L, Sindzingre P (1997) Phys Rev B 56:2521
29. Waldtmann C, Everts H-U, Bernu B, Lhuillier C, Sindzingre P, Lecheminant P, Pierre L (1998) Eur Phys J B 2:501
30. Mila F (1998) Phys Rev Lett 81:2356
31. Mambrini M, Mila F (2000) Eur Phys J B 17:651
32. Subrahmanyam V (1995) Phys Rev B 52:1133

33. Raghu C, Rudra I, Ramasesha S, Sen D (2000) Phys Rev B 62:9484
34. Bernu B, Lhuillier C, Pierre L (1992) Phys Rev Lett 69:2590
35. Sindzingre P, Lhuillier C, Fouet JB (2003) Int J Mod Phys B 17:5031 (cond-mat/0110283)
36. Calandra M, Sorella S (2000) Phys Rev B 61:R11894
37. Capriotti L (2001) Int J Mod Phys B 15:1799
38. Limot L, Mendels P, Collin G, Mondelli C, Ouladdiaf B, Mutka H, Blanchard N, M. Mekata M (2002) Phys Rev B 65:144447 and references therein
39. Budnik R, Auerbach A (2004) Phys Rev Lett 93:187205
40. Budnik R, M.Sc. thesis, Technion, Haifa (2004).